Journal of Medicinal Chemistry Article

J. Med. Chem. **2010,** *53,* 1067–1075 **1067**
DOI: 10.1021/jm9012455

Potent Inhibitors of Furin and Furin-like Proprotein Convertases Containing Decarboxylated P1 Arginine Mimetics

Gero L. Becker,[†] Frank Sielaff,[†] Manuel E. Than,[‡] Iris Lindberg,[§] Sophie Routhier,[∥] Robert Day,[∥] Yinghui Lu,[⊥] Wolfgang Garten,[⊥] and Torsten Steinmetzer*[,†]

[†]*Institute of Pharmaceutical Chemistry, Philipps University Marburg, Marbacher Weg 6, D-35032 Marburg, Germany,* [‡]*Leibniz Institute for Age Research—Fritz Lipmann Institute (FLI), Protein Crystallography Group, Beutenbergstrasse 11, 07745 Jena, Germany,* [§]*Department of Anatomy and Neurobiology, University of Maryland, Baltimore, Maryland 21201,* [∥]*Institut de Pharmacologie de Sherbrooke, Université de Sherbrooke, Sherbrooke, Québec, Canada, J1H 5N4, and* [⊥]*Institute of Virology, Philipps University Marburg, Hans-Meerwein-Strasse 2, 35043 Marburg, Germany*

Received August 19, 2009

Furin belongs to the family of proprotein convertases (PCs) and is involved in numerous normal physiological and pathogenic processes, such as viral propagation, bacterial toxin activation, cancer, and metastasis. Furin and related furin-like PCs cleave their substrates at characteristic multibasic consensus sequences, preferentially after an arginine residue. By incorporating decarboxylated arginine mimetics in the P1 position of substrate analogue peptidic inhibitors, we could identify highly potent furin inhibitors. The most potent compound, phenylacetyl-Arg-Val-Arg-4-amidinobenzylamide (**15**), inhibits furin with a K_i value of 0.81 nM and has also comparable affinity to other PCs like PC1/3, PACE4, and PC5/6, whereas PC2 and PC7 or trypsin-like serine proteases were poorly affected. In fowl plague virus (influenza A, H7N1)-infected MDCK cells, inhibitor **15** inhibited proteolytic hemagglutinin cleavage and was able to reduce virus propagation in a long-term infection test. Molecular modeling revealed several key interactions of the 4-amidinobenzylamide residue in the S1 pocket of furin contributing to the excellent affinity of these inhibitors.

Introduction

Furin is a member of the group of proprotein convertases (PCs), a family of Ca^{2+}-dependent multidomain mammalian endoproteases that contain a catalytic serine protease domain of the subtilisin type.[1] Together with six other members of this family, PC2, PC1/3, PACE4, PC4, PC5/6, and PC7, furin possesses a strong preference for substrates containing the multibasic cleavage motif Arg-X-Arg/Lys-Arg↓-X.[2−4]

Furin and its analogues are responsible for the maturation of a huge number of inactive protein precursors[5,6] and are therefore involved in many normal physiological processes. However, several studies have also revealed a function of these proteases in numerous diseases, such as viral and bacterial infections, tumorigenesis, neurodegenerative disorders, diabetes, and atherosclerosis.[3,4] For instance, furin-like PCs can process the HIV-1 surface protein gp160 into gp120 and gp41, which form an envelope complex necessary for the virulence of HIV-1.[7] Additional potential substrates are surface proteins of highly pathogenic avian influenza viruses of the H5 and H7 subtypes, from the hemorrhagic Ebola and Marburg viruses or from the measles virus that all must be cleaved at multibasic consensus sites for formation of their mature and fusogenic envelope glycoproteins.[8−11] Furin is also involved in the pathogenicity of *Bacillus anthracis* because of its ability to activate the protective antigen precursor, one component of anthrax toxin.[12] Early endosomal furin also activates several other bacterial toxins, such as *Pseudomonas* exotoxin, Shiga-like toxin-1, and diphtheria toxins.[4] Upregulation of PCs was observed in many tumors, and in some cases, elevated levels of PC expression could be correlated with enhanced malignancy and invasiveness, probably via activation of metalloproteases, angiogenic factors, growth factors, and their receptors.[13−16] However, the function of PCs in the regulation of tumor growth and progression seems to be more complex, because other reports describe that PCs are also involved in the activation of proteins with tumor suppressor functions, such as cadherins.[17] PCs are involved in neurodegenerative disorders such as Alzheimer's disease by activation of α-, β-, and γ-secretases or via the release of amyloidogenic peptides.[18] The intracellular endoproteolytic PC-catalyzed activation of membrane-bound MT1-MMP in macrophages is important for plaque stability in atherosclerosis.[19] The cleavage efficacy of the PCs toward a large number of potential substrates, some of which are likely to be involved in additional diseases, has been recently investigated in detail.[5] Therefore, PC inhibitors might represent potential drugs for the treatment of these diseases.

Compared to other arginine-specific proteases, such as the trypsin-like serine proteases thrombin and factor Xa, only moderate progress has been achieved in the field of PC inhibitors. PCs are inhibited by various naturally occurring macromolecular protein-based inhibitors; additional bio engineered inhibitors have been designed by incorporation of the PC's consensus sequence into variants of the serpin α1-antitrypsin, the leech-derived eglin C, and the third domain

*To whom correspondence should be addressed: Institute of Pharmaceutical Chemistry, Philipps University Marburg, Marbacher Weg 6, D-35032 Marburg, Germany. Telephone: +49-6421-2825900. Fax: +49-6421-2825901. E-mail: steinmetzer@staff.uni-marburg.de.

Published on Web 12/28/2009

of turkey ovomucoid.[20,21] Most of the small molecule PC inhibitors belong to three groups, pure peptides, peptide mimetics, or nonpeptidic compounds. Peptides derived from the PC prodomains[22] or identified from a combinatorial library inhibit furin and some related PCs in the micromolar range.[23] Improved activity was obtained with polyarginine[24] or poly-D-arginine-derived analogues; the most potent compound, nona-D-arginine, inhibits furin with a K_i value of 1.3 nM.[25] The first potent peptidomimetic furin inhibitors were developed by coupling of appropriate multibasic substrate sequences to a P1 arginyl chloromethyl ketone group. The irreversible inhibitor decanoyl-Arg-Val-Lys-Arg-CMK has now been used by many groups as a reference to study the effects of furin and related PCs.[9] Other groups developed ketone-based transition state analogues, which most likely inhibit furin via formation of a reversible hemiketal.[26] Although these ketone-derived inhibitors are valuable biochemical tools, especially for X-ray analysis[27] and for preliminary in vivo studies (for example, with fowl plaque virus[8]), they are less suited for drug design. Ketones are often prone to racemization at the P1 Cα and can be attacked by numerous nucleophiles, which limits their stability in vivo.[28] A boroarginine-derived transition state inhibitor was used for the determination of the crystal structure of Kex2, a furin analogue protease from yeast.[29]

Excellent potency was described for a series of nonpeptidic multibasic 2,5-dideoxystreptamine derivatives, which inhibit furin with K_i values of < 10 nM and have negligible affinity to trypsin-like serine proteases.[30] Very recently, several nonpeptidic inhibitors with micromolar affinities were identified by high-throughput screening.[31]

In the past several years, numerous groups have developed substrate analogue inhibitors for trypsin-like serine proteases containing decarboxylated P1 arginine mimetics, e.g., for the clotting proteases thrombin[32,33] and factor Xa.[34] Such analogues are not susceptible to degradation by carboxypeptidases and do not contain a negatively charged P1 carboxylate group, which should repel the inhibitor from the serine nucleophile in the enzyme's active site. Therefore, we incorporated some of these P1 residues in tetrapeptide derivatives derived from furin's consensus sequence and could identify the 4-amidinobenzylamide group as an excellent arginine replacement. Herein, we report the activity of these compounds on furin inhibition; for selected compounds, we also describe their specificity toward the PC family and certain trypsin-like serine proteases. A model in complex with furin reveals several interactions of the P1 group that might contribute to the excellent potency of these compounds. One inhibitor was used to inhibit the replication of a highly pathogenic avian influenza virus (HPAIV)[a] of subtype H7 in a cellular assay.

Results

Chemistry. A combined solution- and solid-phase approach was used for inhibitor synthesis. All compounds containing a symmetric P1 diamine moiety as well as their guanylated analogues (**3**−**12**) were prepared on trityl chloride resin by standard Fmoc SPPS. Initially, the resin was loaded with the diamine, followed by coupling of the P2−P5 residues. The peptides were cleaved from resin to yield the unprotected amines. These were finally modified by treatment with 1*H*-pyrazole-1-carboxamidine[35] in a mixture of a Na_2CO_3 solution with DMF (Scheme 1).

Scheme 1. Synthesis of Inhibitors **3**−**8**[a]

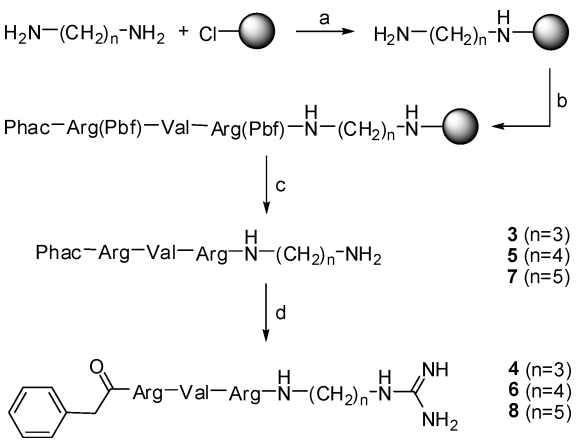

[a] Reagents and conditions: (a) trityl chloride resin, 2 equiv of diamine, dry THF, 2 h; (b) Fmoc SPPS, double couplings with 4 equiv of amino acid (or phenylacetic acid), HOBt and HBTU, respectively, and 8 equiv of DIPEA; (c) TFA/TIS/H_2O (95/2.5/2.5, v/v/v), 2 h; (d) 3 equiv of 1*H*-pyrazole-1-carboxamidine·HCl, 4 equiv of DIPEA in a DMF/1 M Na_2CO_3 solution (1/1, v/v), 16 h.

The P5−P2 segments of inhibitors **13**−**18** were prepared by standard Fmoc SPPS on 2-chlorotrityl chloride resin (Scheme 2). After liberation of the side chain-protected intermediate **2** from resin, 4-amidinobenzylamine·2HCl (**1**) was coupled in solution using a PyBOP/DIPEA mixture in the presence of excess Cl-HOBt. Final side chain deprotection provided inhibitor **15**. In analogy, 1-Boc-4-(aminomethyl)piperidine was coupled to fragment **2**, followed by cleavage of protecting groups to yield **13**, which was converted by treatment with 1*H*-pyrazole-1-carboxamidine and DIPEA to inhibitor **14**. The synthesis of compounds **16**−**18** was performed in analogy to that of inhibitor **15**, using decanoic or acetic acid in the final coupling step.

Determination of Inhibition Constants. Our initial work was focused on the identification of a more druglike P1 residue to replace the arginine ketone moieties used in previously described furin inhibitors. The peptide sequence of the inhibitors was derived from the chloromethyl ketone decanoyl-Arg-Val-Lys-Arg-CMK,[7] whereas the P2 residue was changed to arginine to prevent a second guanylation of an unprotected Lys side chain during reactions with 1*H*-pyrazole-1-carboxamidine, which would lead to homoarginine derivatives. In addition, the N-terminal decanoyl group was substituted with a hydrophobic phenylacetyl group to facilitate UV detection, especially when intermediates without aromatic systems were to be analyzed on HPLC, e.g., analogues with aliphatic diamines in P1 position. The structures of the inhibitors synthesized are summarized in Table 1.

Initially, we incorporated an agmatine moiety in the P1 position, which directly corresponds to a decarboxylated arginine. As described for substrate analogue thrombin inhibitors, we also prepared the shorter and longer analogues[36] and purified their corresponding amines (e.g., **5**),

[a] Abbreviations: Ac, acetyl; Amba, 4-amidinobenzylamide; Cbz, carboxybenzyl; DCM, dichloromethane; Dec, decanoyl; DIPEA, diisopropylethylamine; DMF, dimethylformamide; ER, endoplasmic reticulum; FCS, fetal calf serum; FPV, fowl plaque virus; HA, all forms of the hemagglutinin; HBTU, *O*-benzotriazolyl-*N*,*N*,*N*′,*N*′-tetramethyluronium hexafluorophosphate; HOBt, hydroxybenzotriazole; HPAIV, highly pathogenic avian influenza virus; LPAI, low-pathogenic or apathogenic influenza virus strains; MDCK, Madin-Darby canine kidney; PDB, Protein Data Bank; PFU, plaque-forming units; Phac, phenylacetyl; PyBOP, (benzotriazolyl)-*N*-oxy-pyrrolidinium phosphonium hexafluorophosphate; SPPS, solid-phase peptide synthesis; TFA, trifluoroacetic acid; TIS, triisopropylsilane; THF, tetrahydrofuran.

Scheme 2. Synthesis of Inhibitors **13**−**15**[a]

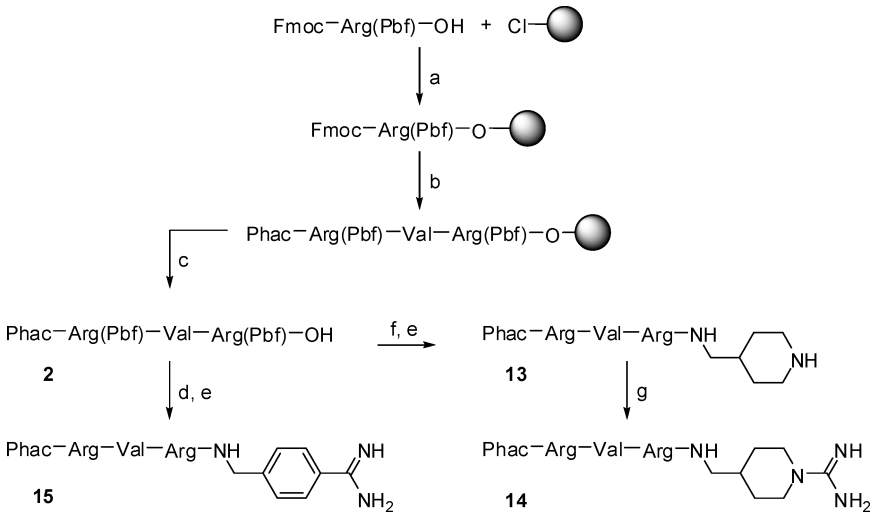

[a] Reagents and conditions: (a) loading of 2-chlorotrityl chloride resin, Fmoc-Arg(Pbf)-OH, 4 equiv of DIPEA, dry DCM, 2 h; (b) Fmoc SPPS (for conditions, see Scheme 1); (c) 1% TFA in DCM, 2 × 30 min; (d) **1**, 1.1 equiv of PyBOP, 3 equiv of 6-Cl-HOBt, 3 equiv of DIPEA in DMF, 2 h; (e) TFA/TIS/H_2O (95/2.5/2.5, v/v/v), 2 h; (f) 1-Boc-4-(aminomethyl)piperidine, 1.1 equiv of PyBOP, 3 equiv of 6-Cl-HOBt, 3 equiv of DIPEA in DMF, 2 h; (g) 3 equiv of 1*H*-pyrazole-1-carboxamidine·HCl, 4 equiv of DIPEA in DMF, 16 h.

which were obtained as intermediates directly after cleavage from resin. A similar inhibitory potency toward furin was observed for the agmatine (**6**) and noragmatine (**4**) derivatives, whereas their analogue amines are significantly less potent and have K_i values of >1 μM. In contrast, for the longer diaminopentane inhibitor **7**, a slightly stronger potency compared to that of its guanylated analogue **8** was found. A poor potency was observed for both diaminoxylene inhibitors and their guanylated analogues (**9**−**12**), whereas the *N*-(amidino)piperidine-derived inhibitor **14** binds to furin with a K_i value of 53 nM. In preliminary investigations, we could find only a poor inhibition of furin with simple benzamidine and 4-aminomethylbenzamidine (**1**) with inhibition constants of 0.75 and 1.2 mM, respectively. Therefore, we were delighted to observe excellent potency with 4-amidinobenzylamide compound **15**. Enzyme kinetic studies revealed that all compounds summarized in Table 1 act as reversible competitive inhibitors; as an example, the Dixon plot for inhibitor **15** is given in Figure 1.

For comparison to the reference inhibitor Dec-Arg-Val-Lys-Arg-CMK, we also prepared analogues with N-terminal decanoyl and acetyl groups and a P2 Lys derivative. Whereas slightly reduced potency was observed for decanoyl compound **16**, an excellent K_i value was found for acetylated inhibitor **17**. P2 Lys inhibitor **18** has activity comparable to that of its Arg analogue **16**, which indicates that both residues are well accepted by furin's S2 pocket.

Although some differences in substrate specificity exist between furin-like PCs,[5] they all share a strong preference for similar multibasic cleavage sequences. Therefore, we assumed that these substrate analogue inhibitors also have the potential to inhibit other PCs. To prove this hypothesis, we selected five compounds and measured their selectivity toward related PCs (Table 2).

As expected, other PCs, such as hPACE4, hPC5/6, and hPC2, were also inhibited in a similar range by the selected inhibitors, whereas hPC7 and hPC2 were less affected. Surprisingly, the highest potency for hPC2 was observed with decanoyl analogue **16**. To further analyze selectivity, three inhibitors with different P1 residues were also tested toward the trypsin-like serine proteases thrombin, factor Xa, and plasmin; however, only a marginal inhibition of these proteases was found.

Inhibition of Proteolytic Hemagglutinin (HA) Cleavage of Fowl Plague Virus (FPV). The virus surface HA-spike protein of FPV, which belongs to the highly pathogenic avian influenza (HPAI) viruses of subtypes H5 and H7, is synthesized as precursor molecule HA0. HA0 is cleaved by furin or by a furin-like protease, present in all cells, at a multibasic cleavage site into distal subunit HA1 and membrane-anchored subunit HA2. The cleavage occurs during the transport of HA from the ER to the plasma membrane, where virus assembly and budding take place.[37,38] At the beginning of infection, after receptor binding and endocytosis, the viral envelope merges with the endosomal membrane. The viral genome and accessory proteins are delivered into the cell nucleus, where multiplication of influenza virus progeny proceeds. The fusion step is essential for each host cell infection cycle and is absolutely dependent on correctly cleaved HA. However, it should be mentioned that cleavage is not required for hemagglutination or virus assembly. We selected inhibitor **15** to study its effects on the proteolytic processing of HA0 in FPV-infected cells (Figure 2). FPV-infected cell cultures were exposed to different concentrations of inhibitor **15** and Dec-Arg-Val-Lys-Arg-CMK, which was used as a control. When viruses in the cell supernatant reached a hemagglutination titer of 2^7 HAU, cell lysates were prepared and viral proteins analyzed. The level of cleavage of HA is most reduced with both inhibitors at a concentration of 50 μM (Figure 2A). Stepwise 2-fold dilution of the inhibitors is associated with a gradual loss of noncleaved HA0, which was quantified by using a near-IR dye-labeled antibody. The IC_{50} value of compound **15** is approximately 10 μM and is in a range similar to that found for the control inhibitor (Figure 2B). Very similar results in this cellular assay were also obtained with decanoyl inhibitor **16**, whereas acetyl analogue **17** had reduced activity (data not shown). At 50 μM concentrations of inhibitor **15**, the virus particles obtained from inhibitor-treated cells contain considerable ($>80\%$) noncleaved HA (data not shown).

Table 1. Inhibition of Furin by Inhibitors of the General Formula R-Arg-Val-P2-P1

Inhibitor	R	P2	P1	K_i (nM)
3	Phac	Arg	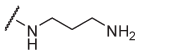	3020
4	Phac	Arg	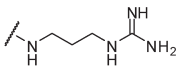	63
5	Phac	Arg	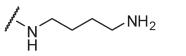	7490
6	Phac	Arg	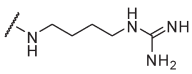	78
7	Phac	Arg	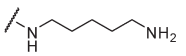	553
8	Phac	Arg	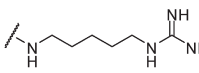	1070
9	Phac	Arg	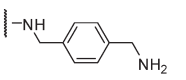	627
10	Phac	Arg	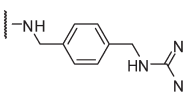	1430
11	Phac	Arg	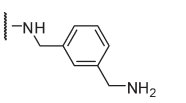	1320
12	Phac	Arg	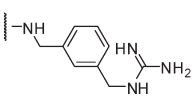	2730
13	Phac	Arg	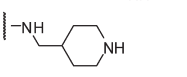	9710
14	Phac	Arg	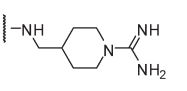	53
15	Phac	Arg	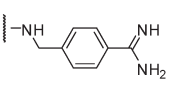	0.81
16	Dec	Arg	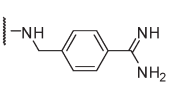	1.6
17	Ac	Arg	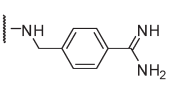	1.0
18[a]	Dec	Lys	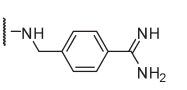	3.3

[a] This compound was synthesized according to Scheme 2 using Fmoc-Lys(Cbz)-OH for coupling of the P2 amino acid. The Cbz group was removed in the final step by hydrogenation in 90% acetic acid at room temperature overnight using Pd/C as a catalyst.

Multiple-Cycle Replications of FPV in the Presence and Absence of Inhibitors. Inhibitory effects on long-term virus infection were examined by multiple-cycle replication of FPV after an inoculation of the cell cultures with a low multiplicity of infection (MOI). This type of experiment results in a retardation and reduced virus replication in the presence of inhibitors.[39] MDCK cells were infected by FPV at a low MOI of 10^{-5} and incubated in the presence of 25 μM compound **15** and in the absence of any inhibitor for up to 72 h. FPV propagation in the presence of compound **15** at 25 μM was monitored by virus titration of released virus into the cell culture supernatants using the standard hemagglutination test[39] (Figure 3). Virus release appears delayed by ~24 h in comparison to that in FPV-infected cell cultures which were not treated with inhibitor and in which FPV has more rapidly proliferated. The fact that FPV is still produced after a period of delay up to nearly the same level as obtained without inhibitor demonstrates that the viability of the cells is not noticeably influenced in the presence of inhibitor.

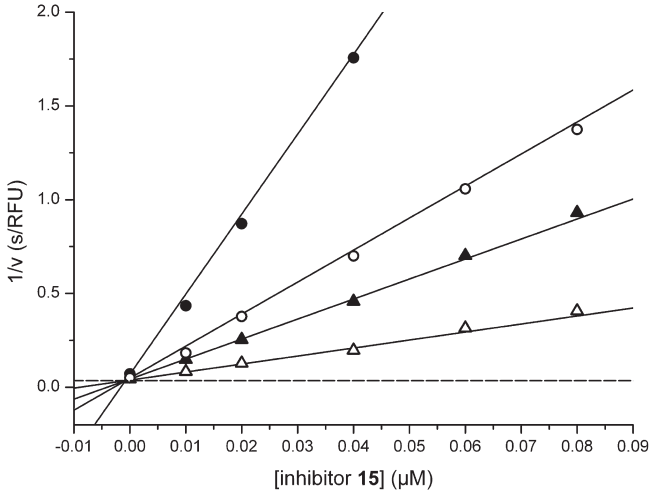

Figure 1. Dixon plot of inhibitor **15**. Kinetic measurements were performed with four different substrate (pyroGlu-Arg-Thr-Lys-Arg-AMC) concentrations [(●) 5, (○) 12.5, (▲) 20, and (△) 50 μM] in the presence of 0.95 nM furin using various inhibitor concentrations of ≥10 nM. The dashed line represents $1/V_{max}$, which was obtained from a Michaelis−Menten curve measured at the same time in parallel on the same 96-well plate (K_m = 4.9 μM; V_{max} = 28.4 RFU/s).

Discussion

A search for suitable replacements of the P1 arginylketones in a series of peptidic furin inhibitors revealed various alternatives among decarboxylated arginine mimetics, known from previous developments of trypsin-like serine protease inhibitors. The incorporation of 4-amidinobenzylamide, originally used for the development of the thrombin inhibitor melagatran and of its hydroxyamidino prodrug ximelagatran,[32] noragmatine,[40] agmatine,[36] and 4-(amidomethyl)-*N*-(amidino)piperidine,[41] provided potent inhibitors of furin and related PCs, such as hPACE4, hPC5/6, and hPC2. The limited selectivity toward the PC family might be a drawback of these inhibitors under some circumstances but otherwise could provide some advantage for special applications, i.e., if PCs are coexpressed in cells and the inhibition of only one PC may not be sufficient. The low affinity of the selected inhibitors toward thrombin, factor Xa, and plasmin, which is in the range of simple benzamidines, should be advantageous for the maintenance of the homeostasis of blood without affecting the well-balanced clotting and fibrinolysis systems. One of the reasons for the

Table 2. Specificity of Selected Inhibitors for Furin-like PCs and Trypsin-like Serine Proteases

	K_i (nM)								
inhibitor	furin	hPACE4	hPC5/6	hPC7	hPC1/3	hPC2	thrombin	fXa	plasmin
6	78	42	85	> 10000	53	> 10000	102000	83000	97000
14	53	67	173	> 10000	70	> 10000	50000	123000	> 1000000
15	0.81	0.6	1.6	6154	0.75	312	23000	40000	6000
16	1.6	3.0	6.3	968	3.65	55	nd[a]	nd[a]	nd[a]
17	1.0	2.4	3.6	5131	1.7	1388	nd[a]	nd[a]	nd[a]

[a] Not determined.

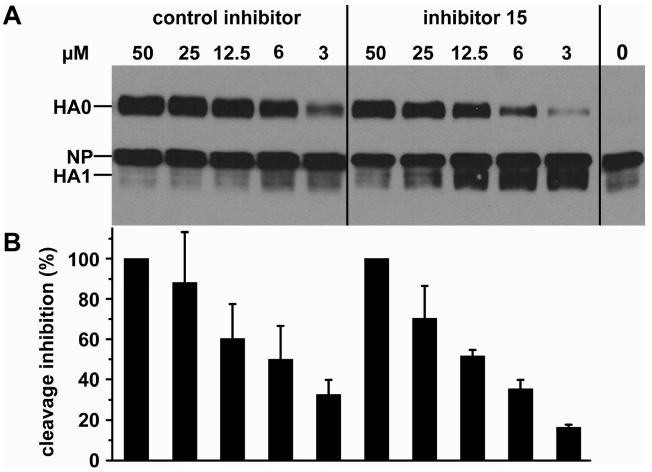

Figure 2. Inhibition of fowl plague virus hemagglutinin cleavage by compound **15** and Dec-Arg-Val-Lys-Arg-CMK as a control. (A) Confluent MDCK cell cultures were infected with egg-grown influenza virus A/FPV/Rostock/34 (H7N1) at a multiplicity of infection of 10 per cell. Inhibition of HA cleavage (PSKKRK-KR↓GLFG) at different inhibitor concentrations was analyzed after cell lysis 16 h postinfection. Proteins from virus-infected cells were subjected to SDS−PAGE and Western blotting. Viral proteins were immunochemically detected by using rabbit anti-FPV serum and the ECL reaction kit (Pierce): HA0 (82 kDa), nucleoprotein NP (56 kDa), and HA1 (~50 kDa). HA2 (32 kDa) was not detectable by the antiserum used. (B) Quantification of HA cleavage inhibition. Three independent experiments for both inhibitors were performed using a modified Western blot analysis technique allowing quantification by a near-IR dye-labeled second monoclonal antibody applicable for the LI-COR Odyssey Image System. The maximum amount of HA0 obtained by inhibition with 50 μM Dec-Arg-Val-Lys-Arg-CMK was normalized to 100% cleavage inhibition. Other HA0 band intensities at different concentrations were measured and equalized by standardization of each HA0 value correlating with the corresponding nucleoprotein NP band (56 kDa).

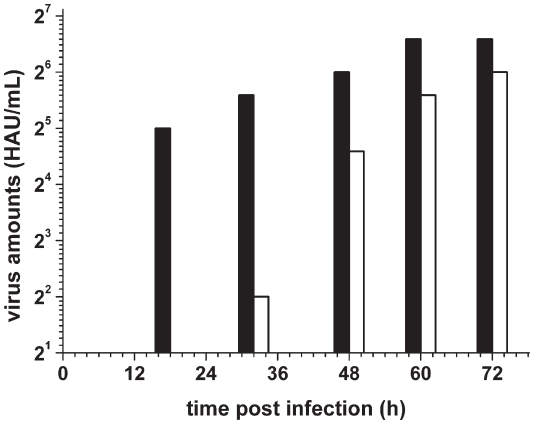

Figure 3. Inhibition of multiple-cycle replication of FPV in cell culture in the absence (black bars) and in the presence of inhibitor **15** (white bars). Cultures of MDCK cells were inoculated with the Rostock strain of FPV at an MOI of 10^{-5} PFU per cell and incubated in DMEM without FCS at 37 °C. The inhibitor was added to the medium, reaching a final concentration of 25 μM. At different times (10, 18, 32, 48, 60, and 72 h postinfection), the amount of virus released into the medium was measured by hemagglutination titration (HAU), and at 10 h, no released virus was detected in either group. Mean values of four independent experiments are shown.

different affinities toward PCs and trypsin-like proteases is most likely the different requirements for the configuration of the P3 residue. Most of the potent noncovalent substrate analogue trypsin-like serine protease inhibitors contain a P3 residue in the D-configuration, whereas the PC inhibitors described here possess an L-amino acid at this position.

Very often, peptidic structures suffer from poor stability due to rapid proteolysis. However, because of the missing C-terminal carboxyl group, we assume that the inhibitors described in Table 1 are resistant to cleavage by carboxypeptidases, whereas the N-terminal acetylation should stabilize them against aminopeptidases. However, at present, we have no information regarding the stability of these compounds toward endoproteases.

To gain a first idea regarding the binding mode of the 4-amidinobenzylamide in the S1 pocket, we modeled the complex of inhibitor **18** bound to furin, based on the known X-ray structure of mouse furin in complex with the irreversible inhibitor Dec-Arg-Val-Lys-Arg-CMK.[27] Therefore, we replaced the arginyl-chloromethyl ketone group in PDB entry 1p8j with 4-amidinobenzylamide followed by energy minimization. As only three amino acid residues vary between the catalytic domains of the mouse and human enzymes, none being in the proximity of the catalytic cleft, the modeled complex between inhibitor **18** and the mouse enzyme should also be representative of the human enzyme (Figure 4).

On the basis of the modeled structure, we could identify several interactions between the P1 residue and furin which may explain the high potency of the 4-amidinobenzylamide inhibitors. The amidino group binds to the carbonyl oxygen of Ala292 and makes salt bridges to the carboxyl side chains of Asp306 and Asp258. In addition, a weak hydrogen bond is formed between the carbonyl oxygen of Pro256 and the surrounding water molecules, connecting the amidinobenzyl moiety via the Ca^{2+} ion to the carboxyl side chains of Glu331 and Asp301. The benzyl ring is sandwiched between the main chains of Trp254 and Gly255 and the main chains of Gly294 and Asn295, similar to the guanidino group of the P1 Arg seen in the experimental structure. Several other hydrogen bonds are formed between the enzyme and the inhibitor, which are identical to the X-ray structure. The P2 Lys amino group binds to the carboxyl residue of Asp154, to the side chain amide of Asn192, and weakly to the carbonyl of Asp191. In addition, hydrogen bonds are formed to a cluster of water

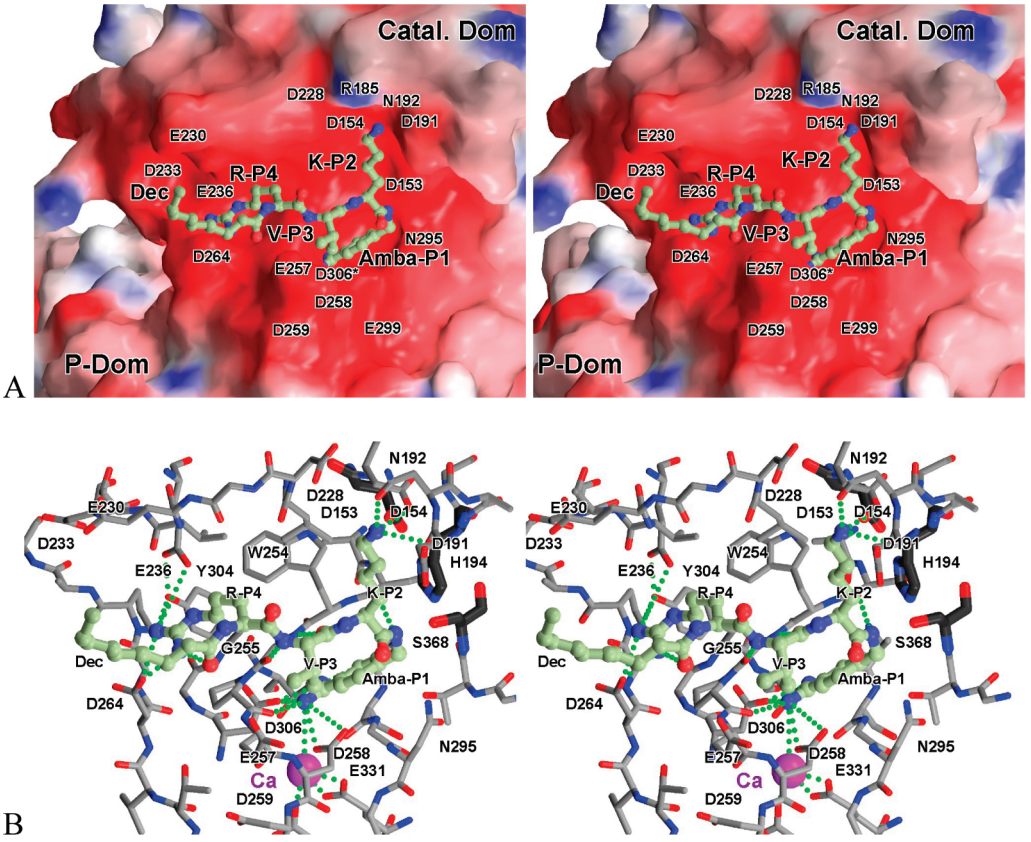

Figure 4. Stereoview of the modeled complex between inhibitor **18** (Dec-Arg-Val-Lys-Amba) and mouse furin. (A) The inhibitor (ball-and-stick model) is shown in front of the solid surface of the catalytic domain, colored according to its calculated negative (−15 e/kT, red) and positive (15 e/kT, blue) electrostatic potential. Most of the amino acids responsible for the strong negative surface potential in the vicinity of the active site are labeled. Asp306 (denoted with an asterisk) is actually located below the enzyme surface at the bottom of the S1 pocket, making a direct contact with the amidino moiety of the inhibitor (see also panel B). (B) Stick model of the surrounding residues together with the inhibitor (ball-and-stick model, carbon colored light green). Furin carbons are colored gray, oxygens red, and nitrogens blue. The catalytic residues are shown as thicker dark gray sticks, and the calcium 2 ion at the bottom of the S1 pocket is shown as a purple sphere. For the sake of clarity, water molecules were omitted and only important enzyme residues involved in interactions with the inhibitor and/or being responsible for the strong negative surface potential are labeled. Strong H-bond and salt bridge contacts discussed in the text are indicated by dotted green lines. Panel B was slightly rotated with respect to panel A to improve the visibility. A PDB file of the modeled complex is available as Supporting Information. This figure was prepared using Grasp,[50] MolScript,[51] and Raster3D.[52]

molecules. A P2 Arg side chain should easily be accommodated by a slight rearrangement of those water molecules and, again after a slight structural rearrangement, potentially by additional interaction(s) with the carboxyl side chains of Asp228 and Asp191. The backbone of the P3 Val forms a short antiparallel β-sheet to Gly255, reminiscent of similar interactions between the D-P3 residue in trypsin-like serine protease inhibitors and the protease residue Gly216. However, in the case of substrate analogue furin inhibitors, an L-configuration of the P3 residue is required, because the space above the indole ring of Trp254 is filled by the side chain of Leu227 and is therefore not accessible for the side chain of a P3 amino acid in the D-configuration. The β-sheet mentioned above is completed by a hydrogen bond between the P1 amide NH group and the carbonyl group of Ser253. The NH group and carbonyl oxygen of the P4 Arg and the decanoyl carbonyl group are involved in hydrogen bonds with surrounding water molecules, bridging interaction with the amide NH group of Glu257. The P4 guanidine group makes salt bridges to Asp264 and Glu236. It forms additional tight hydrogen bonds with the carbonyl oxygen of its own P5 residue and the OH group of Tyr308, connecting it again with the carboxyl side chain of Glu236.

These newly described inhibitors should be useful tools for further studies of the physiological role of furin-like PCs. In a first application, compound **15** inhibited the multiple-cycle replication of FPV in cell culture and suppressed the activation of HA precursor HA0 in FPV-infected cells with a potency similar to that observed for the chloromethyl ketone-based control inhibitor. However, in contrast to the nanomolar K_i values, a significantly higher inhibitor concentration of approximately 10 μM was required in the cellular assay to produce a 50% inhibition of HA0 cleavage. The reduced potency could be related to the predominant intracellular localization of furin within the trans-Golgi network,[42] which makes the protease poorly accessible to such multibasic and polar inhibitors. A strong discrepancy between the potent in vitro activity and significantly reduced efficacy in cellular assays was also found for many other furin inhibitors.[25,30,43−45] In contrast, relatively small differences were determined for a recently discovered series of more hydrophobic dicoumarols; the obtained IC_{50} values from cellular assays were only slightly increased compared to their K_i values, which were in the range between 1 and 20 μM.[31]

Despite equipotent activity between inhibitor **15** and the chloromethyl ketone inhibitor, we believe that the 4-amidinobenzylamide derivatives have a significant advantage because of their improved stability. We could not detect any change in the elution profile of inhibitor **15** by HPLC, when a stock

solution of the inhibitor was stored in water at room temperature over a period of 2 weeks. The synthesis and incorporation of the chemically stable 4-amidinobenzylamide group into peptidic inhibitors are less laborious than the preparation of arginyl ketone derivatives. Therefore, a more simple optimization of these PC inhibitors will be possible in the future. Our work is presently focused on the design of inhibitors with different selectivity profiles and improved physicochemical properties, including the use of well-known benzamidine prodrug strategies, to enhance cell permeability and bioavailability. We assume that these are important prerequisites for further enhancing the activity of the 4-amidinobenzylamide-derived furin inhibitors in cellular assays and identification of suitable candidates for evaluation in animal models.

Experimental Section

Analytical HPLC experiments were performed on a Shimadzu LC-10A system [column, Nucleodur C_{18}, 5 μm, 100 Å, 4.6 mm × 250 mm (Machery-Nagel, Düren, Germany)] with a linear gradient of acetonitrile (from 1 to 70% over 69 min, detection at 220 nm) containing 0.1% TFA at a flow rate of 1 mL/min. The final inhibitors were purified to >95% purity (detection at 220 nm) by preparative HPLC (pumps, Varian PrepStar model 218 gradient system; detector, ProStar model 320; fraction collector, Varian model 701) using a C_8 column [Nucleodur, 5 μm, 100 Å, 32 mm × 250 mm (Macherey-Nagel)] and a linear gradient of acetonitrile containing 0.1% TFA at a flow rate of 20 mL/min. All inhibitors were finally obtained as TFA salts after lyophilization. The molecular mass of the synthesized compounds was determined using a QTrap 2000 ESI spectrometer (Applied Biosystems). The ^{1}H and ^{13}C NMR spectra were recorded on an ECX-400 instrument (Jeol Inc.) at 400 and 100 MHz, respectively, and are referenced to internal solvent signals.

Reagents for synthesis (Fmoc amino acids, coupling reagents, and reagents for synthesis) were obtained from Orpegen, Novabiochem, Iris, Fluka, Aldrich, or Acros. The automated solid-phase peptide synthesis was performed in a Syro 2000 instrument (MultiSynTech GmbH, Witten, Germany).

4-Amidinobenzylamine·2HCl (1). Ten grams (32 mmol) of Boc-4-acetylhydroxyamidinobenzylamide[34] was dissolved in 500 mL of 90% acetic acid and treated with 650 mg of catalyst (10% Pd/C) under an atmosphere of hydrogen. The mixture was hydrogenated over a period of 48 h; the catalyst was removed by filtration, and the solvent was removed in vacuo. The remaining Boc-4-amidinobenzylamide·acetate was dissolved in 150 mL of water and treated with 40 mL of concentrated HCl. After the mixture had been stirred for 1.5 h at room temperature (RT), the solvent was removed in vacuo and the residue was lyophilized from water: white solid (yield, 6.8 g, 30.6 mmol); MS calcd m/z 149.09, found m/z 150.0, $(M + H)^+$; ^{1}H NMR (400 MHz, D_2O) δ 4.46 (s, 2 H), 7.80−8.01 (2d, 4 H, aromatic); ^{13}C NMR (100 MHz, D_2O) δ 42.64 (CH_2), 128.65, 129.26, 129.62, 138.69 (aromatic), 166.47 (carbon amidino group).

Phac-Arg(Pbf)-Val-Arg(Pbf)-OH (2). Fmoc-Arg(Pbf)-OH (1.509 g, 2.325 mmol, 1 equiv) was dissolved in 15 mL of dry DCM and 1.548 mL (9.3 mmol, 4 equiv) of DIPEA, and the mixture was immediately poured onto 2-chlorotrityl chloride resin (1.5 g, 1 equiv, resin loading of 1.55 mmol/g). The mixture was shaken for 2 h at RT followed by treatment with a DCM/MeOH/DIPEA mixture (17/2/1, v/v/v, 3 × 1 min), washed several times with DCM, DMF, and DCM, and dried in vacuo. The synthesis proceeded by manual Fmoc SPPS using a 4-fold excess of Fmoc-amino acid, HOBt and HBTU, respectively, and 8 equiv of DIPEA. The phenylacetic acid was coupled in accordance with the amino acids. The protected peptide was cleaved from the resin with 1% TFA in DCM (2 × 30 min) at RT. The solvent was removed in vacuo and the peptide lyophilized from 80% *tert*-BuOH in water: white solid (yield, 1.452 g, 1.38 mmol); purity >97% based on HPLC at 220 nm; retention time, 64.6 min; MS calcd m/z 1051.49, m/z found 1052.5, $(M + H)^+$.

Phac-Arg-Val-Arg-3-(amido)propylamine·3TFA (3). 1,3-Diaminopropane (50.03 μL, 0.6 mmol, 4 equiv) was dissolved in 1.2 mL of dry THF and poured immediately onto trityl chloride resin (0.1 g, resin loading of 1.5 mmol/g). The mixture was shaken for 2 h at RT, followed by treatment with a DCM/MeOH/DIPEA mixture (17/2/1, v/v/v, 3 × 1 min), and was washed several times with DCM, DMF, and DCM. The synthesis proceeded by automated Fmoc SPPS as described for the manual synthesis of compound **2**. The product was cleaved by shaking the resin in a TFA/TIS/H_2O mixture (95/2.5/2.5, v/v/v) for 2 h at RT, followed by filtration and precipitation with cold ether. The precipitate was washed twice with ether and dried. The product was purified by preparative HPLC and lyophilized from 80% *tert*-BuOH in water: white solid (yield, 39 mg, 0.041 mmol); retention time, 22.2 min; MS calcd m/z 603.4, found m/z 604.6, $(M + H)^+$.

The synthesis of inhibitors **5**, **7**, **9**, and **11** was performed in an identical manner; for analytical data, see the Supporting Information.

Phac-Arg-Val-Arg-3-(amido)propylguanidine·3TFA (4). To obtain compound **4**, the corresponding amine was prepared via the manner described for compound **3**. The precipitated amine was dissolved in a mixture of 1 mL of a 1 M Na_2CO_3 solution/DMF mixture (1/1, v/v) followed by addition of 1*H*-pyrazole-1-carboxamidine·HCl (68.1 mg, 0.45 mmol) and DIPEA (106 μL, 0.6 mmol). The mixture was stirred for 16 h at RT, and the solvent was removed in vacuo. The residue was purified by preparative HPLC and lyophilized from 80% *tert*-BuOH in water: white solid (yield, 40 mg, 0.041 mmol); retention time, 23.4 min; MS calcd m/z 645.4, found m/z 646.5, $(M + H)^+$.

The synthesis of inhibitors **6**, **8**, **10**, and **12** was performed by an identical procedure; for analytical data, see the Supporting Information.

Phac-Arg-Val-Arg-4-(amidomethyl)piperidine·3TFA (13). Compound **2** (105.2 mg, 0.1 mmol, 1 equiv), 1-Boc-4-(aminomethyl)piperidine (Fluka, 21.43 mg, 0.1 mmol, 1 equiv), PyBOP (57.3 mg, 0.11 mmol, 1.1 equiv), 6-Cl-HOBt (20.9 mg, 0.3 mmol, 3 equiv), and DIPEA (51.36 μL, 0.3 mmol, 3 equiv) were dissolved in 0.5 mL of DMF, and the mixture was stirred for 2 h at RT. The solvent was removed in vacuo to yield a brownish oil. This was dissolved in a TFA/TIS/H_2O mixture (95/2.5/2.5, v/v/v), stirred for 3 h at RT, precipitated with cold ether, washed twice with ether, and dried. The precipitate was purified by preparative HPLC and lyophilized from 80% *tert*-BuOH in water: white solid (yield, 55 mg, 0.056 mmol); retention time, 23.1 min; MS calcd m/z 643.43, found m/z 644.5, $(M + H)^+$.

Phac-Arg-Val-Arg-4-(amidomethyl)-*N*-amidinopiperidine·3TFA (14). Compound **13** (25 mg, 0.02 mmol, 1 equiv) and 1*H*-pyrazole-1-carboxamidine·HCl (9.8 mg, 0.06 mmol, 3 equiv) were dissolved in 0.5 mL of DMF and DIPEA (10.03 μL, 0.08 mmol, 4 equiv). The mixture was stirred for 16 h at RT. The solvent was removed in vacuo, and the product was purified by preparative HPLC and lyophilized from 80% *tert*-BuOH in water: white solid (yield, 19.5 mg, 0.019 mmol); retention time, 24.4 min; MS calcd m/z 685.45, found m/z 343.9, $(M + 2H)^{2+}$.

Phac-Arg-Val-Arg-4-(amidomethyl)benzamidine·3TFA (15). Compound **2** (105.2 mg, 0.1 mmol, 1 equiv), compound **1** (22.21 mg, 0.1 mmol, 1 equiv), PyBOP (57.3 mg, 0.11 mmol, 1.1 equiv), 6-Cl-HOBt (20.9 mg, 0.3 mmol, 3 equiv), and DIPEA (51.36 μL, 0.3 mmol, 3 equiv) were dissolved in 0.5 mL of DMF, and the mixture was stirred for 2 h at RT. After completion of the reaction (HPLC control), the solvent was removed in vacuo to give a brownish oil. The synthesis was continued in a manner similar to that described for compound **13**: white solid (yield, 70 mg, 0.069 mmol); retention time, 24.2 min; MS calcd m/z 678.41, found m/z 679.4, $(M + H)^+$.

The synthesis of inhibitors **16**−**18** was performed as described for **15** using decanoic or acetic acid for coupling of the P5 residue. Inhibitor **18** was prepared by coupling of Fmoc-Lys-(Cbz)-OH as the P2 residue; the Cbz group was removed in the final step by hydrogenation in 90% acetic acid at room temperature overnight using Pd/C as a catalyst. For analytical data, see the Supporting Information.

Enzyme Kinetics with Furin. The inhibition constants of recombinant soluble human furin[25] were determined at RT according to the method of Dixon[46] using a Safire 2 fluorescence plate reader (Tecan) (λ_{ex} = 380 nm; λ_{em} = 460 nm) and pyroGlu-Arg-Thr-Lys-Arg-AMC as the substrate (Bachem) in 100 mM HEPES buffer (pH 7.0) containing 0.2% Triton X-100, 2 mM $CaCl_2$, 0.02% sodium azide, and 1 mg/mL BSA. The enzyme concentration used in the assay was 0.95 nM, and the substrate concentrations were normally 5, 20, and 50 μM; for inhibitor **15**, a fourth substrate concentration of 12.5 μM was used (Figure 1). The lowest inhibitor concentration was at least 10 times higher than the enzyme concentration used to avoid tight binding conditions.

Information about enzyme kinetic studies with PC2, PC1/3, PACE4, PC5/6, and PC7 is given in the Supporting Information. The K_i values for the trypsin-like serine proteases thrombin, factor Xa, and plasmin were determined from Dixon plots as described previously.[47]

Modeling. Inhibitor **18** was manually docked into the active site cleft of furin and energy-minimized using MAIN.[48] Basically, the P1 arginine group of the Dec-Arg-Lys-Arg-CMK-inhibited mouse furin crystal structure (PDB entry 1p8j)[27] was replaced with 4-amidinobenzylamide, and the entire inhibitor was locally energy-minimized using a force field based on the parameters of Engh and Huber[49] while the amidino moiety was kept coplanar with the benzyl ring and the coordinates of the enzyme and the Ca^{2+} ion were rigidly retained. During minimization, the P4 Arg side chain was forced to retain its crystallographically clearly defined conformation (but apparently somewhat unfavored by the force field), as previously described.[27]

Acknowledgment. This work was supported by the Deutsche Forschungsgemeinschaft (SFB 593 TPB2 and TH 862/1-4), by NIH (DA05084 to I. Lindberg) and by grants from the Canadian Institutes of Health Research (CIHR) and the Ministère du Développement économique, de l'Innovation et de l'Exportation (MDEIE) to RD. We thank Petra Neubauer-Rädel for excellent technical assistance and Sarah Fehling for data analysis of the cell assays.

Supporting Information Available: A table containing MS and HPLC data of all final inhibitors, conditions of enzyme kinetic studies with PC2, PC1/3, PACE4, PC5/6, and PC7, conditions of cellular assays for detecting virus inhibition, and a PDB file of inhibitor **18** modeled in complex with mouse furin. This material is available free of charge via the Internet at http://pubs.acs.org.

References

(1) van de Ven, W. J.; Voorberg, J.; Fontijn, R.; Pannekoek, H.; van den Ouweland, A. M.; van Duijnhoven, H. L.; Roebroek, A. J.; Siezen, R. J. Furin is a subtilisin-like proprotein processing enzyme in higher eukaryotes. *Mol. Biol. Rep.* **1990**, *14*, 265–275.
(2) Rockwell, N. C.; Krysan, D. J.; Komiyama, T.; Fuller, R. S. Precursor processing by kex2/furin proteases. *Chem. Rev.* **2002**, *102*, 4525–4548.
(3) Fugere, M.; Day, R. Cutting back on pro-protein convertases: The latest approaches to pharmacological inhibition. *Trends Pharmacol. Sci.* **2005**, *26*, 294–301.
(4) Thomas, G. Furin at the cutting edge: From protein traffic to embryogenesis and disease. *Nat. Rev. Mol. Cell Biol.* **2002**, *3*, 753–766.
(5) Remacle, A. G.; Shiryaev, S. A.; Oh, E. S.; Cieplak, P.; Srinivasan, A.; Wei, G.; Liddington, R. C.; Ratnikov, B. I.; Parent, A.; Desjardins, R.; Day, R.; Smith, J. W.; Lebl, M.; Strongin, A. Y. Substrate cleavage analysis of furin and related proprotein convertases. A comparative study. *J. Biol. Chem.* **2008**, *283*, 20897–20906.
(6) Izidoro, M. A.; Gouvea, I. E.; Santos, J. A.; Assis, D. M.; Oliveira, V.; Judice, W. A.; Juliano, M. A.; Lindberg, I.; Juliano, L. A study of human furin specificity using synthetic peptides derived from natural substrates, and effects of potassium ions. *Arch. Biochem. Biophys.* **2009**, *487*, 105–114.
(7) Hallenberger, S.; Bosch, V.; Angliker, H.; Shaw, E.; Klenk, H. D.; Garten, W. Inhibition of furin-mediated cleavage activation of HIV-1 glycoprotein gp160. *Nature* **1992**, *360*, 358–361.
(8) Stieneke-Grober, A.; Vey, M.; Angliker, H.; Shaw, E.; Thomas, G.; Roberts, C.; Klenk, H. D.; Garten, W. Influenza virus hemagglutinin with multibasic cleavage site is activated by furin, a subtilisin-like endoprotease. *EMBO J.* **1992**, *11*, 2407–2414.
(9) Garten, W.; Hallenberger, S.; Ortmann, D.; Schafer, W.; Vey, M.; Angliker, H.; Shaw, E.; Klenk, H. D. Processing of viral glycoproteins by the subtilisin-like endoprotease furin and its inhibition by specific peptidylchloroalkylketones. *Biochimie* **1994**, *76*, 217–225.
(10) Volchkov, V. E.; Feldmann, H.; Volchkova, V. A.; Klenk, H. D. Processing of the Ebola virus glycoprotein by the proprotein convertase furin. *Proc. Natl. Acad. Sci. U.S.A.* **1998**, *95*, 5762–5767.
(11) Volchkov, V. E.; Volchkova, V. A.; Stroher, U.; Becker, S.; Dolnik, O.; Cieplik, M.; Garten, W.; Klenk, H. D.; Feldmann, H. Proteolytic processing of Marburg virus glycoprotein. *Virology* **2000**, *268*, 1–6.
(12) Gordon, V. M.; Klimpel, K. R.; Arora, N.; Henderson, M. A.; Leppla, S. H. Proteolytic activation of bacterial toxins by eukaryotic cells is performed by furin and by additional cellular proteases. *Infect. Immun.* **1995**, *63*, 82–87.
(13) Bassi, D. E.; Lopez De Cicco, R.; Mahloogi, H.; Zucker, S.; Thomas, G.; Klein-Szanto, A. J. Furin inhibition results in absent or decreased invasiveness and tumorigenicity of human cancer cells. *Proc. Natl. Acad. Sci. U.S.A.* **2001**, *98*, 10326–10331.
(14) Scamuffa, N.; Siegfried, G.; Bontemps, Y.; Ma, L.; Basak, A.; Cherel, G.; Calvo, F.; Seidah, N. G.; Khatib, A. M. Selective inhibition of proprotein convertases represses the metastatic potential of human colorectal tumor cells. *J. Clin. Invest.* **2008**, *118*, 352–363.
(15) Khatib, A. M.; Bassi, D.; Siegfried, G.; Klein-Szanto, A. J.; Ouafik, L. Endo/exo-proteolysis in neoplastic progression and metastasis. *J. Mol. Med.* **2005**, *83*, 856–864.
(16) Bassi, D. E.; Fu, J.; Lopez de Cicco, R.; Klein-Szanto, A. J. Proprotein convertases: "Master switches" in the regulation of tumor growth and progression. *Mol. Carcinog.* **2005**, *44*, 151–161.
(17) Müller, E. J.; Caldelari, R.; Posthaus, H. Role of subtilisin-like convertases in cadherin processing or the conundrum to stall cadherin function by convertase inhibitors in cancer therapy. *J. Mol. Histol.* **2004**, *35*, 263–275.
(18) Bennett, B. D.; Denis, P.; Haniu, M.; Teplow, D. B.; Kahn, S.; Louis, J. C.; Citron, M.; Vassar, R. A furin-like convertase mediates propeptide cleavage of BACE, the Alzheimer's β-secretase. *J. Biol. Chem.* **2000**, *275*, 37712–37717.
(19) Stawowy, P.; Meyborg, H.; Stibenz, D.; Borges Pereira Stawowy, N.; Roser, M.; Thanabalasingam, U.; Veinot, J. P.; Chretien, M.; Seidah, N. G.; Fleck, E.; Graf, K. Furin-like proprotein convertases are central regulators of the membrane type matrix metalloproteinase-pro-matrix metalloproteinase-2 proteolytic cascade in atherosclerosis. *Circulation* **2005**, *111*, 2820–2827.
(20) Bontemps, Y.; Scamuffa, N.; Calvo, F.; Khatib, A. M. Potential opportunity in the development of new therapeutic agents based on endogenous and exogenous inhibitors of the proprotein convertases. *Med. Res. Rev.* **2007**, *27*, 631–648.
(21) Basak, A. Inhibitors of proprotein convertases. *J. Mol. Med.* **2005**, *83*, 844–855.
(22) Basak, A.; Lazure, C. Synthetic peptides derived from the prosegments of proprotein convertase 1/3 and furin are potent inhibitors of both enzymes. *Biochem. J.* **2003**, *373*, 231–239.
(23) Apletalina, E.; Appel, J.; Lamango, N. S.; Houghten, R. A.; Lindberg, I. Identification of inhibitors of prohormone convertases 1 and 2 using a peptide combinatorial library. *J. Biol. Chem.* **1998**, *273*, 26589–26595.
(24) Cameron, A.; Appel, J.; Houghten, R. A.; Lindberg, I. Polyarginines are potent furin inhibitors. *J. Biol. Chem.* **2000**, *275*, 36741–36749.
(25) Kacprzak, M. M.; Peinado, J. R.; Than, M. E.; Appel, J.; Henrich, S.; Lipkind, G.; Houghten, R. A.; Bode, W.; Lindberg, I. Inhibition of furin by polyarginine-containing peptides: Nanomolar inhibition by nona-D-arginine. *J. Biol. Chem.* **2004**, *279*, 36788–36794.
(26) Angliker, H. Synthesis of tight binding inhibitors and their action on the proprotein-processing enzyme furin. *J. Med. Chem.* **1995**, *38*, 4014–4018.
(27) Henrich, S.; Cameron, A.; Bourenkov, G. P.; Kiefersauer, R.; Huber, R.; Lindberg, I.; Bode, W.; Than, M. E. The crystal structure of the proprotein processing proteinase furin explains its stringent specificity. *Nat. Struct. Biol.* **2003**, *10*, 520–526.

(28) Powers, J. C.; Asgian, J. L.; Ekici, O. D.; James, K. E. Irreversible inhibitors of serine, cysteine, and threonine proteases. *Chem. Rev.* **2002**, *102*, 4639–4750.
(29) Holyoak, T.; Wilson, M. A.; Fenn, T. D.; Kettner, C. A.; Petsko, G. A.; Fuller, R. S.; Ringe, D. 2.4 Å resolution crystal structure of the prototypical hormone-processing protease Kex2 in complex with an Ala-Lys-Arg boronic acid inhibitor. *Biochemistry* **2003**, *42*, 6709–6718.
(30) Jiao, G. S.; Cregar, L.; Wang, J.; Millis, S. Z.; Tang, C.; O'Malley, S.; Johnson, A. T.; Sareth, S.; Larson, J.; Thomas, G. Synthetic small molecule furin inhibitors derived from 2,5-dideoxystreptamine. *Proc. Natl. Acad. Sci. U.S.A.* **2006**, *103*, 19707–19712.
(31) Komiyama, T.; Coppola, J. M.; Larsen, M. J.; van Dort, M. E.; Ross, B. D.; Day, R.; Rehemtulla, A.; Fuller, R. S. Inhibition of furin/proprotein convertase-catalyzed surface and intracellular processing by small molecules. *J. Biol. Chem.* **2009**, *284*, 15729–15738.
(32) Gustafsson, D.; Bylund, R.; Antonsson, T.; Nilsson, I.; Nystrom, J. E.; Eriksson, U.; Bredberg, U.; Teger-Nilsson, A. C. A new oral anticoagulant: The 50-year challenge. *Nat. Rev. Drug Discovery* **2004**, *3*, 649–659.
(33) Steinmetzer, T.; Stürzebecher, J. Progress in the development of synthetic thrombin inhibitors as new orally active anticoagulants. *Curr. Med. Chem.* **2004**, *11*, 2297–2321.
(34) Schweinitz, A.; Stürzebecher, A.; Stürzebecher, U.; Schuster, O.; Stürzebecher, J.; Steinmetzer, T. New substrate analogue inhibitors of factor Xa containing 4-amidinobenzylamide as P1 residue: Part 1. *Med. Chem.* **2006**, *2*, 349–361.
(35) Bernatowicz, M. S.; Wu, Y.; Matsueda, G. R. 1H-Pyrazole-1-carboxamidine hydrochloride an attractive reagent for guanylation of amines and its application to peptide synthesis. *J. Org. Chem.* **1992**, *57*, 2497–2502.
(36) Wiley, M. R.; Chirgadze, N. Y.; Clawson, D. K.; Craft, T. J.; Giffordmoore, D. S.; Jones, N. D.; Olkowski, J. L.; Schacht, A. L.; Weir, L. C.; Smith, G. F. Serine-protease selectivity of the thrombin inhibitor D-Phe-Pro-agmatine and its homologs. *Bioorg. Med. Chem. Lett.* **1995**, *5*, 2835–2840.
(37) Garten, W.; Klenk, H. D. Cleavage activation of the influenza virus hemagglutinin and its role in pathogenesis. In *Avian Influenza*; Klenk, H. D., Matrosovich, M., Stech, J., Eds.; Karger: Basel, Switzerland, 2008; Vol. 27, pp 156−167.
(38) Klenk, H. D.; Garten, W. Host cell proteases controlling virus pathogenicity. *Trends Microbiol.* **1994**, *2*, 39–43.
(39) Garten, W.; Stieneke, A.; Shaw, E.; Wikstrom, P.; Klenk, H. D. Inhibition of proteolytic activation of influenza virus hemagglutinin by specific peptidyl chloroalkyl ketones. *Virology* **1989**, *172*, 25–31.
(40) Gustafsson, D.; Elg, M.; Lenfors, S.; Borjesson, I.; Teger-Nilsson, A. C. Effects of inogatran, a new low-molecular-weight thrombin inhibitor, in rat models of venous and arterial thrombosis, thrombolysis and bleeding time. *Blood Coagulation Fibrinolysis* **1996**, *7*, 69–79.
(41) Steinmetzer, T.; Batdorsdhjin, M.; Kleinwächter, P.; Seyfarth, L.; Greiner, G.; Reissmann, S.; Stürzebecher, J. New thrombin inhibitors based on D-cha-Pro-derivatives. *J. Enzyme Inhib.* **1999**, *14*, 203–216.
(42) Schäfer, W.; Stroh, A.; Berghofer, S.; Seiler, J.; Vey, M.; Kruse, M. L.; Kern, H. F.; Klenk, H. D.; Garten, W. Two independent targeting signals in the cytoplasmic domain determine trans-Golgi network localization and endosomal trafficking of the proprotein convertase furin. *EMBO J.* **1995**, *14*, 2424–2435.
(43) Jean, F.; Thomas, L.; Molloy, S. S.; Liu, G.; Jarvis, M. A.; Nelson, J. A.; Thomas, G. A protein-based therapeutic for human cytomegalovirus infection. *Proc. Natl. Acad. Sci. U.S.A.* **2000**, *97*, 2864–2869.
(44) Komiyama, T.; VanderLugt, B.; Fugere, M.; Day, R.; Kaufman, R. J.; Fuller, R. S. Optimization of protease-inhibitor interactions by randomizing adventitious contacts. *Proc. Natl. Acad. Sci. U.S.A.* **2003**, *100*, 8205–8210.
(45) Jean, F.; Stella, K.; Thomas, L.; Liu, G.; Xiang, Y.; Reason, A. J.; Thomas, G. α1-Antitrypsin Portland, a bioengineered serpin highly selective for furin: Application as an antipathogenic agent. *Proc. Natl. Acad. Sci. U.S.A.* **1998**, *95*, 7293–7298.
(46) Dixon, M. The determination of enzyme inhibitor constants. *Biochem. J.* **1953**, *55*, 170–171.
(47) Stürzebecher, J.; Prasa, D.; Hauptmann, J.; Vieweg, H.; Wikström, P. Synthesis and structure-activity relationships of potent thrombin inhibitors: Piperazides of 3-amidinophenylalanine. *J. Med. Chem.* **1997**, *40*, 3091–3099.
(48) Turk, D. Weiterentwicklung eines Programmes für Molekülgraphik und Elektronendichte-Manipulation und seine Anwendung auf verschiedene Protein-Strukturaufklärungen. Ph.D. Thesis, Technische Universität München, Munich, Germany, 1992.
(49) Engh, R. A.; Huber, R. Accurate bond and angle parameters for X-ray protein-structure refeinement. *Acta Crystallogr.* **1991**, *A47*, 329–400.
(50) Nicholls, A.; Sharp, K. A.; Honig, B. Protein folding and association: Insights from the interfacial and thermodynamic properties of hydrocarbons. *Proteins* **1991**, *11*, 281–296.
(51) Kraulis, P. J. MOLSCRIPT: A program to produce both detailed and schematic plots of protein structures. *J. Appl. Crystallogr.* **1991**, *24*, 946–950.
(52) Merritt, E. A.; Bacon, D. J. Raster3D: Photorealistic molecular graphics. *Methods Enzymol.* **1997**, *277*, 505–524.